

# Reaction Mechanism of Deamidation of Asparaginyll Residues in Peptides: Effect of Solvent Molecules<sup>†</sup>

Saron Catak,<sup>‡,§</sup> Gérald Monard,<sup>§</sup> Viktoriya Aviyente,<sup>\*,‡</sup> and Manuel F. Ruiz-López<sup>§</sup>

Department of Chemistry, Bogazici University, 34342 Bebek, Istanbul, Turkey, and Equipe de Chimie et Biochimie Théoriques, UMR CNRS-UHP No. 7565, Université Henri Poincaré, BP 239, 54506 Vandoeuvre-lès-Nancy, France

Received: December 1, 2005; In Final Form: April 3, 2006

Deamidation of proteins occurs spontaneously under physiological conditions. Asparaginyll (Asn) residues may deamidate into aspartyl (Asp) residues, causing a change in both the charge and the conformation of peptides. It has been previously proposed by Capasso et al. that deamidation of relatively unrestrained Asn residues proceeds through a succinimide intermediate. This mechanism has been modeled by Konuklar et al. and the rate determining step for the deamidation process in neutral media has been shown to be the cyclization step leading to the succinimide intermediate. In the present study, possible *water-assisted* mechanisms, for both concerted and stepwise succinimide formation, were computationally explored using the B3LYP method with 6-31+G\*\* basis set. Single point solvent calculations were carried out in water, by means of integral equation formalism-polarizable continuum model (IEF-PCM) at the B3LYP/6-31++G\*\* level of theory. A novel route leading to the succinimide intermediate via tautomerization of the Asn side chain amide functionality has been proposed. The energetics of these pathways have been subject to a comparative study to identify the most probable mechanism for the deamidation of peptides in solution.

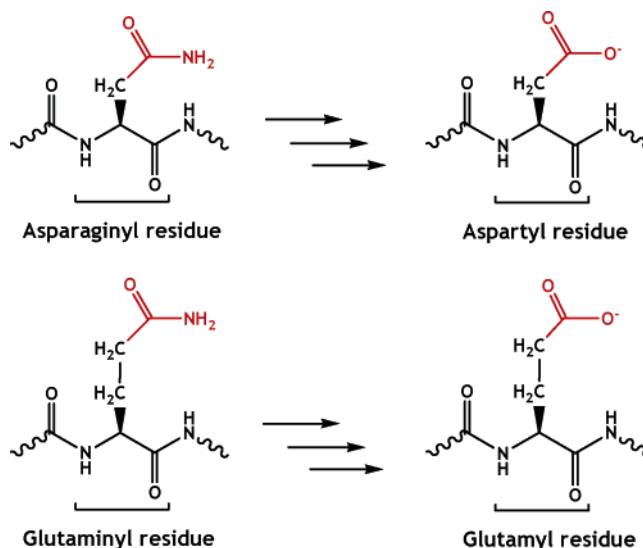
## Introduction

The deamidation of proteins may occur under physiological conditions and is known to limit the lifetime of proteins.<sup>1</sup> Deamidation is the conversion of the amide group on the side chain of an amino acid residue to a carboxylate or carboxylic acid depending on the pH of the medium. Asparagine (Asn) and glutamine (Gln), two of the 20 amino acid residues that ordinarily occur in proteins, are uniquely unstable under physiological conditions; they spontaneously and nonenzymatically deamidate into glutamyl (Glu) and aspartyl (Asp) residues<sup>2</sup> (Scheme 1). Gln deamidation is usually substantially slower than Asn deamidation.

The deamidation of Asn and Gln in peptides and proteins is of significant biological interest. Over 1700 research papers on various aspects of the deamidation of peptides and proteins have been published<sup>3</sup> since the biological importance of deamidation was first emphasized. Deamidation of asparaginyll and glutaminyll residues causes time-dependent changes in charge and conformation of peptides and proteins.<sup>4–6</sup> Deamidation rates of 1371 asparaginyll residues in a representative collection of 126 human proteins have been calculated.<sup>7</sup> Deamidation half-times for these proteins were shown to range from 1 to 1000 days. These rates have suggested that deamidation is a biologically relevant phenomenon in a remarkably large percentage of human proteins.

The timed processes of protein turnover, development, and aging have been suggested as possible roles for deamidation.<sup>8</sup> It has been hypothesized by Robinson et al. that deamidation serves as a molecular clock for the timing of biological processes.<sup>9</sup> The fact that static properties of asparaginyll and

## SCHEME 1: Deamidation of Asparaginyll and Glutaminyll Residues



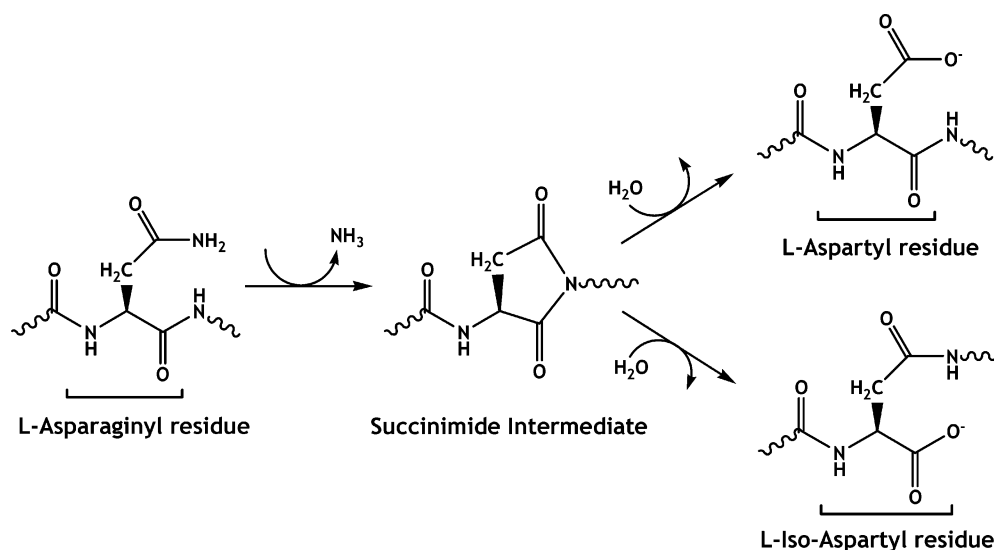
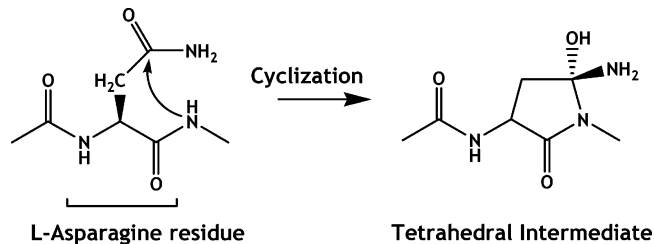
glutaminyll residues are not unique and can be easily duplicated by some of the other 18 commonly occurring amino acid residues suggestively indicates the essence of their disruptive effect on peptide and protein structure by deamidation reactions. Furthermore, it has been proposed by Robinson et al.<sup>9</sup> that the instability of asparaginyll and glutaminyll residues is their primary biological function, and that they serve as easily programmable molecular clocks.

Capasso et al. have proposed that the deamidation of relatively unrestrained Asn residues proceeds through a succinimide intermediate<sup>10–12</sup> (Scheme 2). Acylation of the amino group on the neighboring ( $n + 1$ ) carboxyl side residue by the  $\beta$ -carbonyl

<sup>†</sup> Part of the "Chava Lifshitz Memorial Issue".

<sup>‡</sup> Bogazici University.

<sup>§</sup> Université Henri Poincaré.

SCHEME 2: Deamidation Mechanism Suggested by Capasso et al.<sup>10</sup>SCHEME 3: Rate Determining Step for Deamidation in Neutral Media Suggested by Konuklar et al.<sup>14</sup>

(side chain carbonyl) group of the L-Asn residue produces a five-membered cyclic imide, namely the succinimide intermediate. The first step in the mechanism (Scheme 2) includes the cyclization and consecutive loss of an  $\text{NH}_3$ . The succinimide intermediate then hydrolyzes at either one of the two carbonyls. Experimental findings indicate that the hydrolysis reaction gives L-Asp and L- $\beta$ -Asp (L-iso-Asp) in a 3:1 ratio.<sup>13</sup>

The deamidation of Asn residues via succinimide intermediates has been previously investigated theoretically<sup>14</sup> using density functional theory (B3LYP/6-31G\*). The cyclization, deamination (loss of  $\text{NH}_3$ ) and hydrolysis reactions that lead to the deamidation of a model peptide have been studied and the succinimide intermediate suggested by Capasso et al.<sup>10</sup> has been confirmed. The formation of the succinimide intermediate has been proposed to be a multistep process,<sup>14</sup> in which the initial cyclization step forms a tetrahedral intermediate (Scheme 3). This is followed by the deamination step to produce the succinimide ring. Finally, hydrolysis of the succinimide ring leads to L-Asp or L-iso-Asp residues.<sup>15,16</sup> The rate determining step in neutral media has been proposed to be the formation of the tetrahedral intermediate.<sup>14</sup>

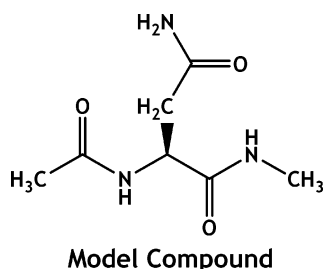
An experimental study has been performed by Robinson et al. on the complete 800-pentapeptide set of all possible combinations of the sequences Gly-Xxx-Asn-Yyy-Gly and Gly-Xxx-Gln-Yyy-Gly, where Xxx and Yyy are any of the 20 normally occurring amino acid residues.<sup>17</sup> This study has indicated that deamidation rate is controlled primarily by the carboxyl side residue (Yyy), also commonly referred to as the  $n + 1$  residue, with smaller effects from the amino side residue (Xxx). This is consistent with the succinimide reaction mechanism that was originally proposed<sup>10</sup> to explain the deamidation rates of Asn-Gly sequences and iso-Asp formation.

In the present study, alternative pathways, namely, *water-assisted* deamidation mechanisms, have been investigated. The effect of explicit  $\text{H}_2\text{O}$  molecules on the mechanism and energetics of deamidation has been explored using computational techniques. Both concerted and stepwise reaction mechanisms leading to the succinimide intermediate have been taken into account. As an alternative mechanism, the tautomerization of the Asn side chain amide functionality has been explored. Activation barriers for these pathways have been used for comparative purposes and to identify the most probable mechanism for deamidation of peptides in solution.

## Computational Methodology

Preliminary analysis of the potential energy surfaces (PES) for all proposed mechanisms were carried out at a semiempirical level (PM3).<sup>18</sup> Further geometry optimizations were performed using the density functional theory (DFT)<sup>19–21</sup> at the B3LYP/6-31+G\*\*<sup>22–24</sup> level of theory. Geometries of stationary points were optimized without any constraints. All stationary points have been characterized by a frequency analysis from which zero-point energy and thermal corrections have also been attained using the ideal gas approximation and standard procedures. Local minima and first order saddle points were identified by the number of imaginary vibrational frequencies. The intrinsic reaction coordinate (IRC) approach,<sup>25,26</sup> followed by full geometry optimization, has been used to determine the species reached by each transition structure. Note that the resulting energy minima do not necessarily correspond to the lowest conformation of the system (particularly for solute–water complexes), though differences are not expected to be large. Free energies of activation ( $\Delta G^\ddagger$ ) are calculated as the difference of free energies between transition states and reactive conformers reached by IRC calculations. All energy values for gas-phase optimized structures listed throughout the discussion include thermal free energy corrections at 298 K and 1 atm.

The effect of a polar environment on the reaction path has been taken into account by use of the self-consistent reaction field (SCRf) theory. Single-point energies in water ( $\epsilon = 78.5$ ) utilizing the integral equation formalism-polarizable continuum (IEF-PCM) model<sup>27–30</sup> at the B3LYP/6-31++G\*\* level were calculated on gas-phase B3LYP/6-31+G\*\* optimized structures. Bondi radii<sup>31</sup> scaled by a factor of 1.2 have been used for solvent calculations. All solvent energies reported include thermal

**SCHEME 4: Model Peptide with L-Asparaginyl Residue**

corrections to free energies, obtained from gas-phase optimizations and nonelectrostatic corrections.

All gas-phase optimizations and single point solvent calculations have been carried out using the Gaussian 03 program package.<sup>32</sup> Reaction mechanisms shown in figures throughout the text contain gas-phase optimized geometries (B3LYP/6-31+G\*\*) of reactive conformers, transition states and products, respectively. All distances shown in the figures are in angstroms (Å).

**Results and Discussion**

In the first part of this study, the succinimide formation mechanism proposed by Capasso et al.<sup>10</sup> and previously modeled by Konuklar et al.<sup>14</sup> has been computationally revisited with a slightly larger model compound (Scheme 4), to more efficiently mimic Asn and its neighboring residues. More specifically, instead of mimicking the backbone NH with an NH<sub>2</sub> group as in the previous model, an acetyl (CH<sub>3</sub>C=O) group has been added to the Asn backbone NH, to help prevent unrealistic intramolecular H-bonding that can be formed by a less restricted NH<sub>2</sub>. In addition, the basis set has been improved by the addition of diffuse functions on heavy atoms and polarization functions on hydrogen atoms, while the method was preserved. The previously suggested concerted mechanism<sup>14</sup> will serve as a benchmark for comparison with energetics of the newly proposed mechanisms in this study.

The previously suggested concerted mechanism has been employed on the new model compound using B3LYP/6-31+G\*\* (Figure 1). This is a four-centered asynchronous concerted mechanism, where the hydrogen on the backbone NH, which belongs to the  $n + 1$  residue, is transferred to the Asn side chain carbonyl group early in the reaction as seen in the

transition state. Later in the concerted step, the backbone nitrogen attacks the carbonyl carbon and the five-membered tetrahedral intermediate forms.

The free energy of activation ( $\Delta G^\ddagger$ ) for this concerted reaction is quite high, 49.7 kcal/mol in the gas phase (40.0 kcal/mol in solution), for a reaction that spontaneously and nonenzymatically occurs under physiological conditions. The same concerted reaction was shown to have an activation barrier of 50.3 kcal/mol in gas phase (47.5 kcal/mol in solution) in the previous study where both a smaller model compound and basis set were used.<sup>14</sup> Hence, there is reason to believe that this reaction may occur through different reaction mechanisms with lower barriers, assisted by solvent molecules that are in the vicinity of the asparaginyl residue.

In the next part of this study, three different reaction mechanisms for the cyclization leading to the tetrahedral intermediate are proposed and computationally explored, all incorporating the effect of explicit H<sub>2</sub>O molecules on the reaction mechanism. In the last part, the deamination mechanism (loss of NH<sub>3</sub>) and the effect of solvent molecules on the reaction barrier and energetics are discussed.

**A. Cyclization. 1. Concerted Water-Assisted Cyclization.** The first water-assisted cyclization mechanism studied is the concerted cyclization step assisted by a single water molecule. The water molecule helps the transfer of the hydrogen from the backbone NH of the  $n + 1$  residue, onto the Asn side chain carbonyl oxygen (Figure 2).

In the optimized geometry for the reactive conformer, the water molecule is shown to form two H-bonds with the model peptide, one with the carbonyl of the Asn side chain, and another with the backbone NH of the neighboring carboxyl side residue. In the transition state structure of this concerted reaction, the hydrogen transfer again takes place early in the transition state and ring closure via attack of backbone  $n + 1$  N to carbonyl C of Asn side chain is observed later in the concerted step.

The energetics of this reaction shows that the concerted reaction can go through a lower barrier with a water-assisted pathway. The water molecule reduces the H...O distance for the proton transfer but has little effect on the C...N distance, thus a slightly reduced but still very high barrier. The free energy of activation for the water-assisted concerted cyclization step is 4.2 kcal/mol (2.9 kcal/mol in solution) lower than that of the concerted reaction (Figure 1).

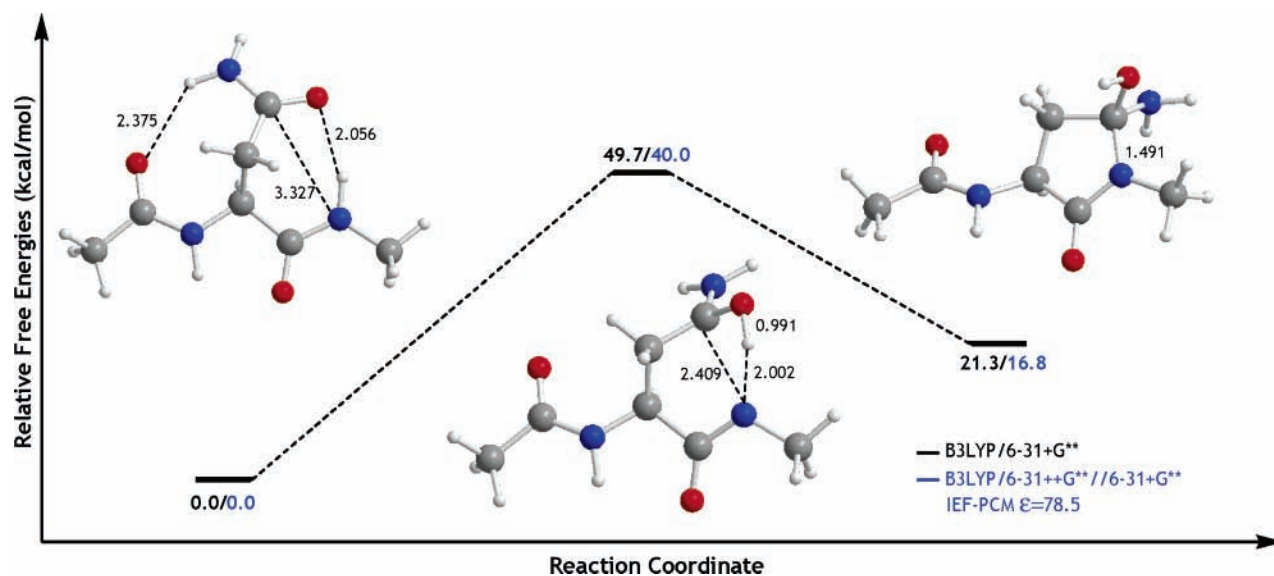


**Figure 1.** Potential free energy profile for the concerted cyclization reaction.

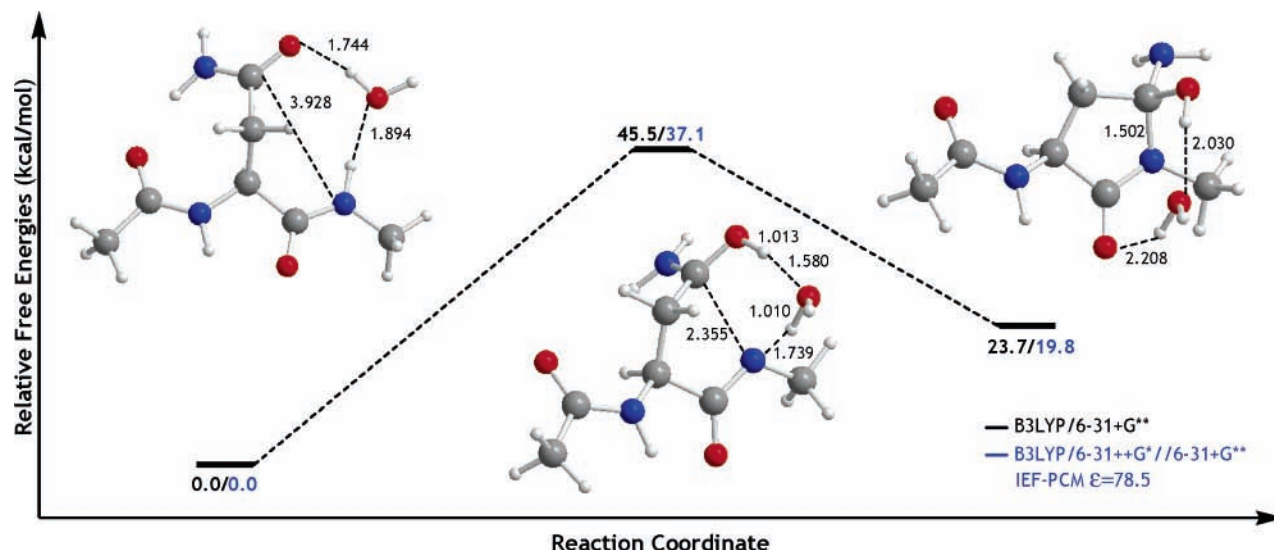


Figure 2. Potential free energy profile for the water-assisted concerted cyclization reaction via 1 H<sub>2</sub>O.

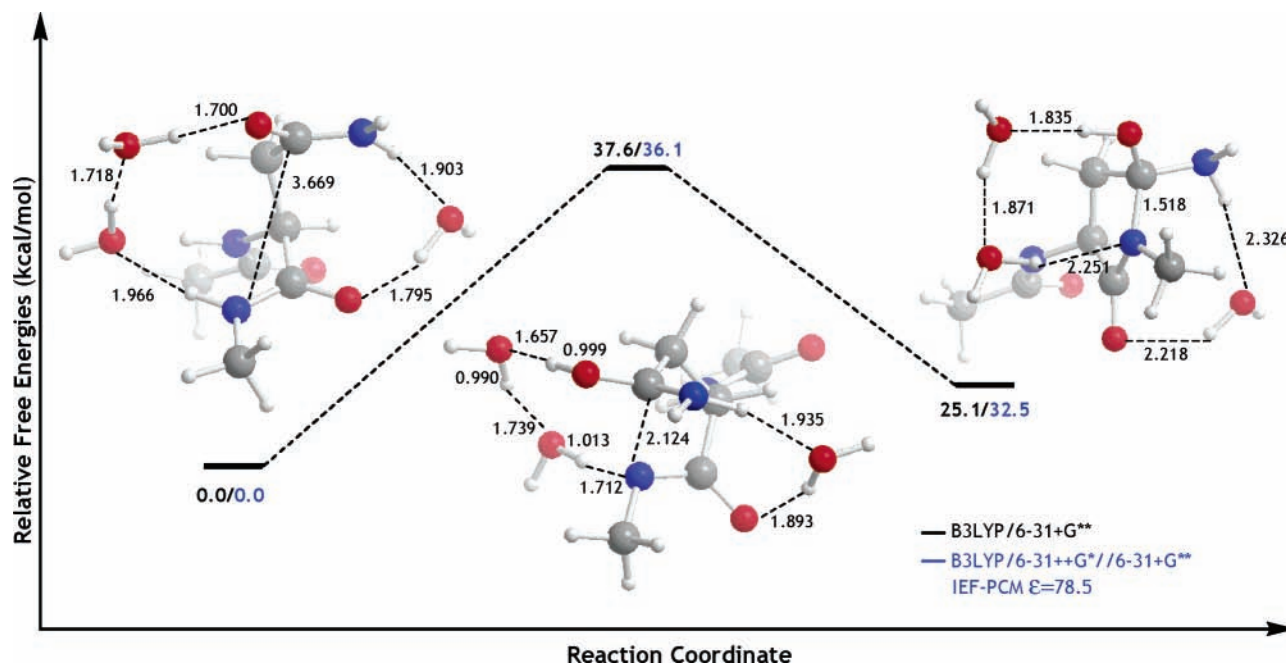


Figure 3. Potential free energy profile for the water-assisted concerted cyclization reaction via 2 active H<sub>2</sub>O molecules.

Another water-assisted concerted cyclization mechanism—assisted by two active H<sub>2</sub>O molecules—has been modeled (Figure 3). In this mechanism, two H<sub>2</sub>O molecules are actively involved in the reaction, while a third H<sub>2</sub>O is in a passive mode. The proton is again transferred from the backbone NH of the carboxyl side residue onto the carbonyl of the Asn side chain; however, this time the proton transfer takes place over two water molecules instead of one. The third water molecule is hydrogen bonded with the Asn backbone carbonyl and the Asn side chain NH<sub>2</sub>, though this water molecule does not actively participate in the reaction, it serves as a stabilizing agent by providing hydrogen bonds.

The free energy of activation for this mechanism is approximately 8 kcal/mol lower than the energy of the one-water-assisted concerted cyclization (Figure 2) and 12.1 kcal/mol lower than that of the originally proposed concerted cyclization (Figure 1). The presence of two water molecules significantly reduces the C—N distance, thus a considerable decrease in the activation barrier is observed.

**2. Stepwise Water-Assisted Cyclization.** The second pathway explored was the water-assisted stepwise cyclization, which consists of two consecutive steps. The first of these steps is the simultaneous deprotonation of the backbone  $n + 1$  NH and protonation of the Asn side chain carbonyl oxygen with the assistance of water molecules. Proton transfer takes place through the water molecules via the hydrogen-bond network. The second step is the ring closure, which involves the negatively charged backbone nitrogen's attack onto the positively charged side chain carbonyl carbon, hence forming the tetrahedral intermediate (Scheme 5).

B3LYP/6-31+G\*\* optimized geometries and free energies for both steps in the water-assisted stepwise cyclization have been modeled (Figure 4). The first barrier shows the proton transfer over two water molecules (deprotonation/protonation). The third water molecule is not actively participating in the reaction; however, it serves as a stabilizing agent, similar to the case in Figure 3. A zwitterionic compound is formed at the end of the first step and is stabilized by H-bonds with water

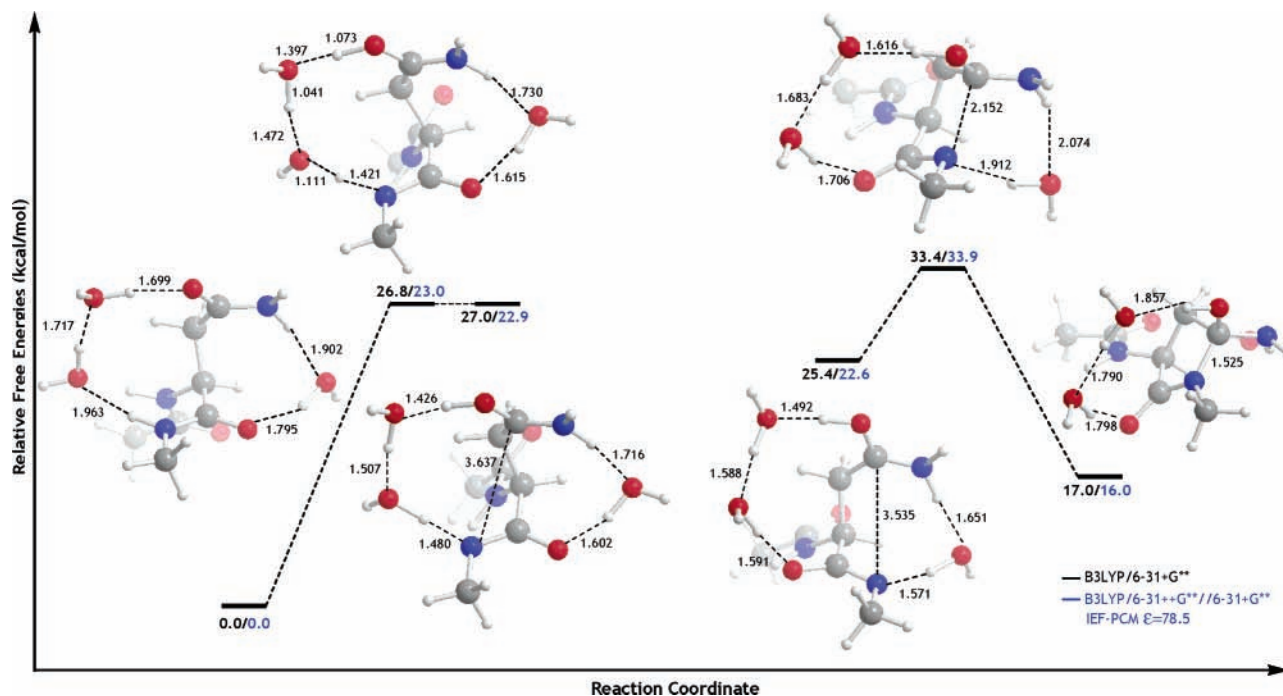
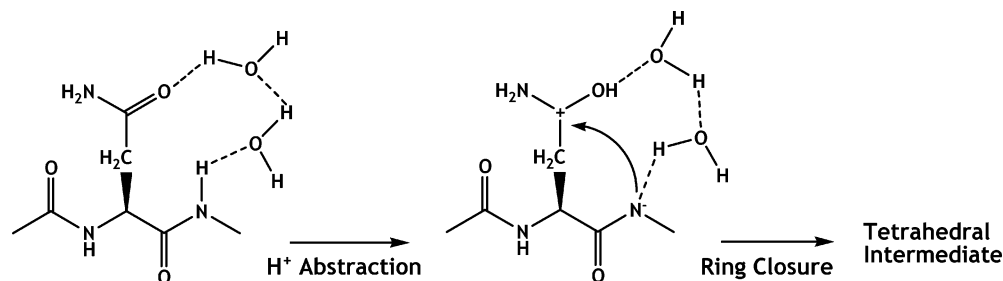


**Figure 4.** Potential free energy profile for the water-assisted stepwise cyclization reaction.

#### SCHEME 5: Mechanism for Stepwise Water-Assisted Cyclization



molecules. The free energy of activation for this step is 26.8 kcal/mol in gas phase. The effect of a polar environment somewhat stabilizes the transition state and free energy of activation in solvent is lower, 23 kcal/mol, for this step.

It should be noted that the attempt to locate the transition state and the product for the deprotonation/protonation step via *one* peripheral water molecule failed. This is possibly due to a very flat potential energy surface between the transition state and the zwitterion formed. A similar case can be seen in the first step of Figure 4, where the transition state and its product have very similar geometries and the potential energy surface is quite flat. This gives us reason to believe that the stepwise cyclization mechanism is not likely to proceed toward the next step but fall back to the reactant. Nevertheless, assuming the zwitterion could be stable enough to complete the ring closure, we have investigated the next step. The formation of the tetrahedral intermediate could not be found starting from the zwitterion formed at the end of the first step. However, by a simple change in the backbone, the zwitterion can be transformed into a reactive conformer. This conformational change is a rotation around the Asn  $C_{\alpha}$ -CO bond to form the reactant of the second step shown in Figure 4. The backbone rotation mentioned has not been modeled in this study, and it has been assumed that it will not affect the overall barrier of the water-assisted stepwise cyclization appreciably, because the two intermediates are very close in energy, the latter being a little more stable.

The second step in the water-assisted cyclization is the ring closure. This step is expected to have a low barrier, because a negatively charged nitrogen atom is attacking a positive carbon; hence the barrier for ring closure alone is 8 kcal/mol in gas phase (12.3 kcal/mol in solution).

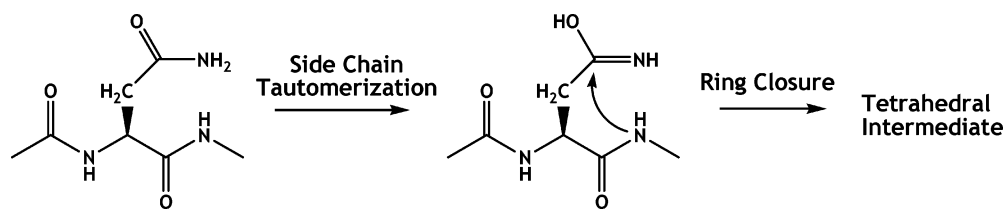
There is an effective H-bond network between the peptide and the three peripheral water molecules throughout the reaction, with H-bond distances ranging from 1.42 to 1.965 Å.

The overall free energy of activation for the water-assisted stepwise cyclization is shown to be 33.4 kcal/mol in gas phase (33.9 kcal/mol in solution). This energy barrier is more than 15 kcal/mol lower than the free energy of activation for the gas phase concerted reaction previously reported.<sup>14</sup> It is also lower in energy than the concerted water-assisted cyclization mechanisms previously discussed in this text.

**3a. Asparagine Side Chain Tautomerization.** The asparagine side chain, like any other amide functionality, can tautomerize into an amidic acid tautomer, with the transfer of a proton from the side chain  $NH_2$  group to the side chain carbonyl oxygen. The tautomerization reaction is depicted together with the ring closure that leads to the tetrahedral intermediate (Scheme 6). This is an alternative pathway leading to the tetrahedral intermediate, which can then be converted to the succinimide intermediate through expulsion of  $NH_3$ .

Side chain tautomerization may occur with or without the assistance of water molecules. Asn side chain tautomerization with no help from surrounding water molecules has been

## SCHEME 6: Asparagine Side Chain Tautomerization Followed by Cyclization to Tetrahedral Intermediate



modeled (Figure 5). This is a four-centered concerted reaction with an expected high  $\Delta G^\ddagger$ , which was calculated to be approximately 45 kcal/mol in the both gas phase and solution. The tautomerization of the amide functional group to the amidic acid tautomer is not likely to proceed through a concerted four-centered reaction but rather through a water-assisted concerted one, where the proton transfer occurs via peripheral water molecules in the vicinity of the amide functionality.

Asn side chain tautomerization through one peripheral water molecule has been explored (Figure 6). The free energy of activation for this reaction is significantly lower than the tautomerization reaction, which lacked the assistance of a water molecule (Figure 5). The water-assisted tautomerization barrier

is less than half the barrier for the four-centered reaction. The proton transfer from the  $\text{NH}_2$  group to the carbonyl group goes through a water molecule, which is initially H-bonded to both functional groups (Figure 6).

Asn side chain tautomerization through two peripheral water molecules (Figure 7) was shown to have an activation barrier slightly lower than the one-water case (Figure 6).  $\Delta G^\ddagger$  values for both the one-water-assisted and two-water-assisted tautomerizations are comparable and their difference with the barrier of Figure 5 indicates the necessity of modeling these reactions with explicit water molecules to better mimic the reaction in solution.

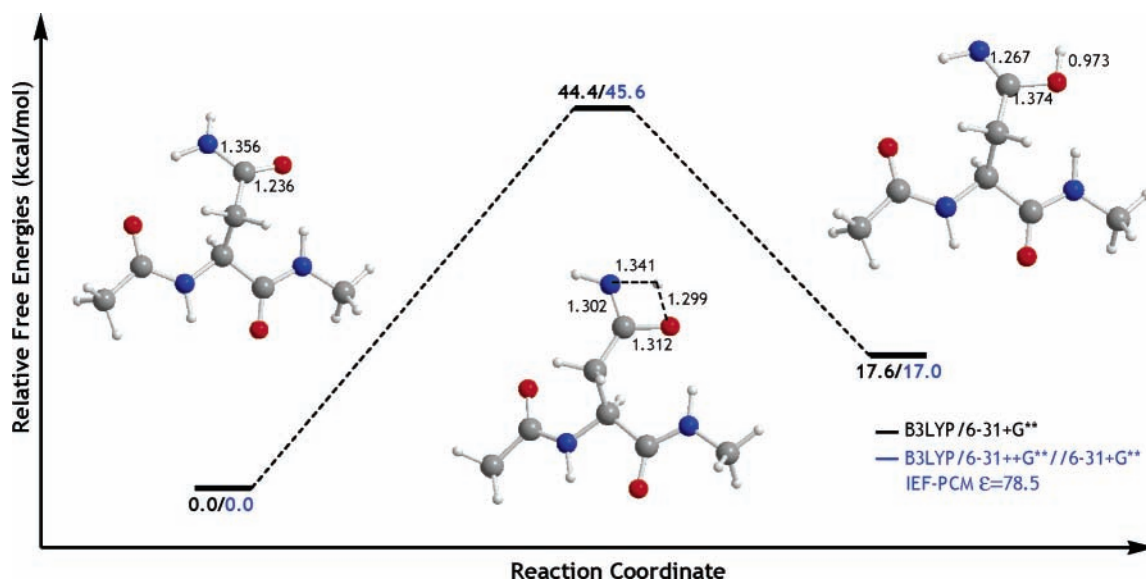


Figure 5. Potential free energy profile for the asparagine side chain tautomerization without explicit  $\text{H}_2\text{O}$  molecule.

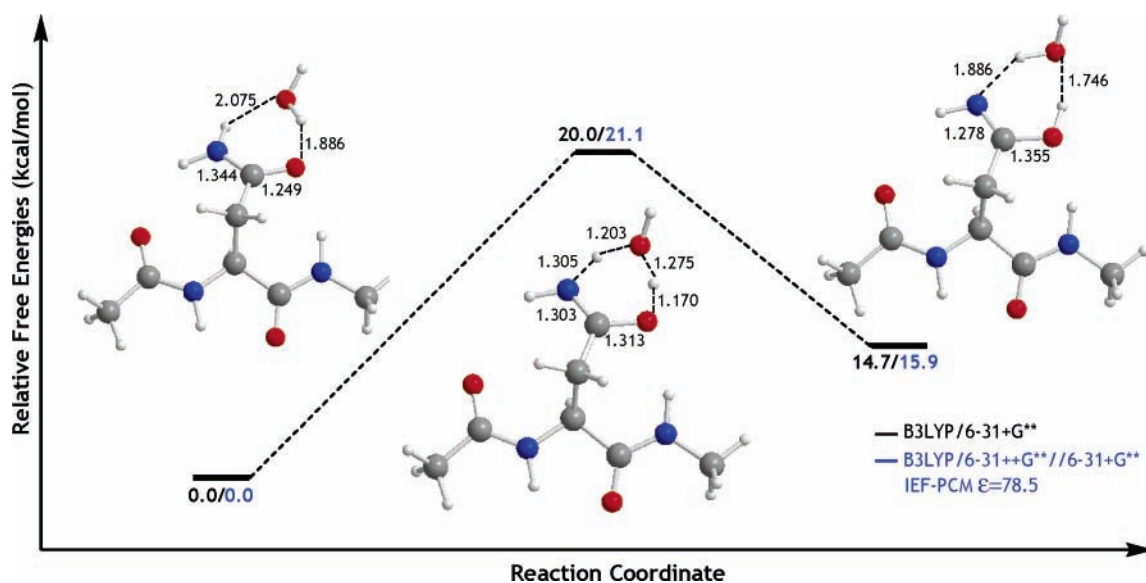


Figure 6. Potential free energy profile for the asparagine side chain tautomerization through 1 peripheral  $\text{H}_2\text{O}$ .

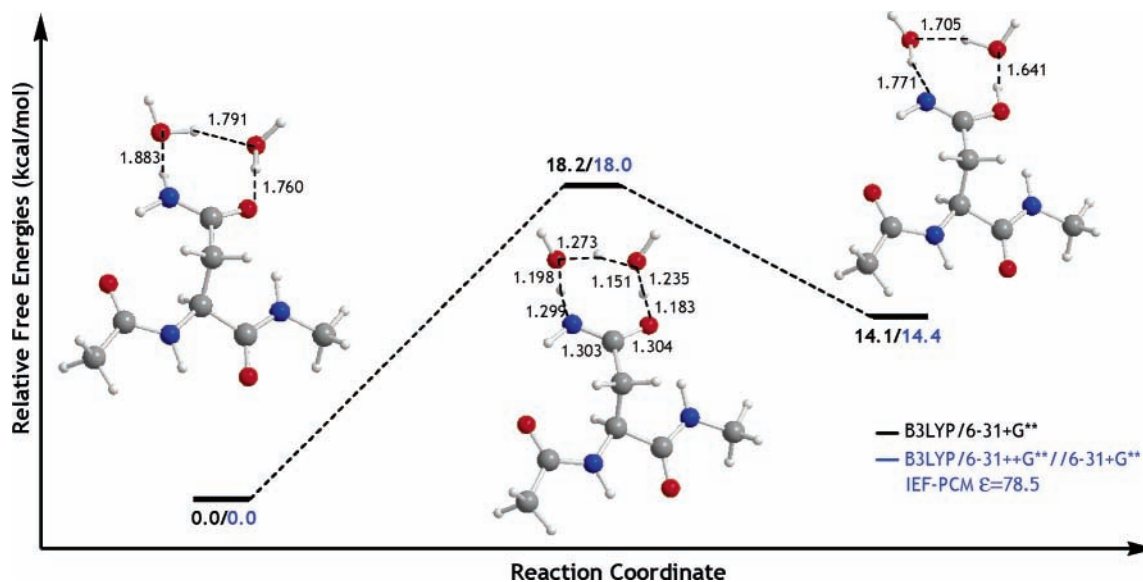


Figure 7. Potential free energy profile for the asparagine side chain tautomerization through 2 peripheral H<sub>2</sub>O.

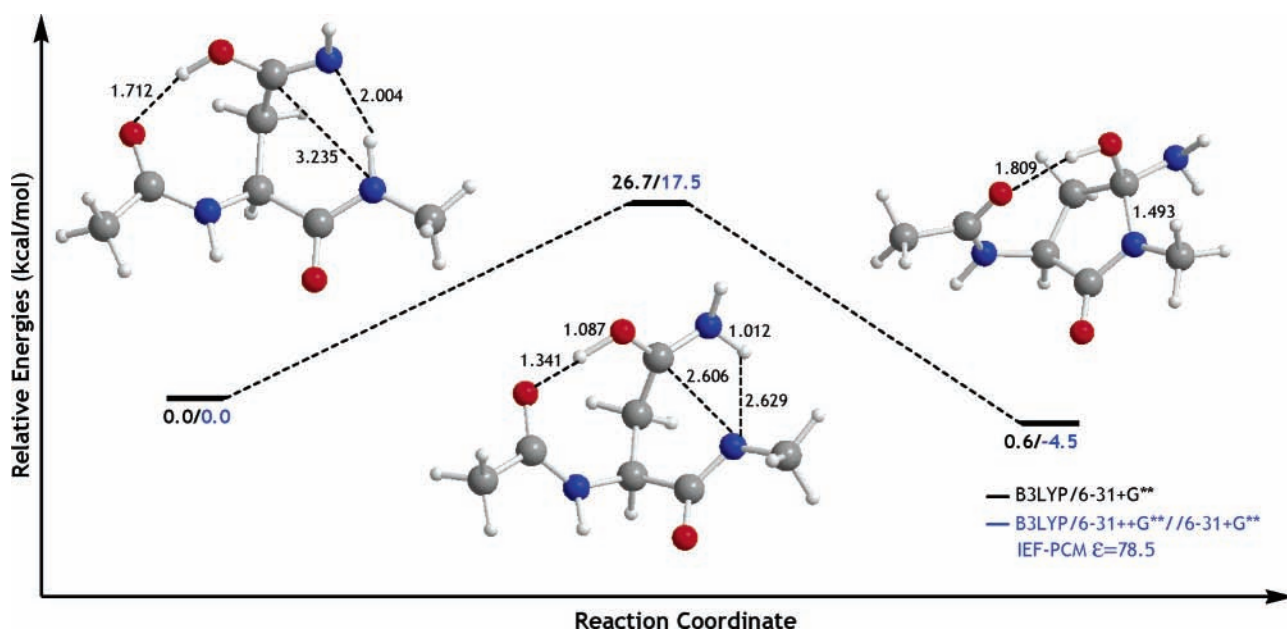


Figure 8. Potential free energy profile for the concerted ring closure in amidic acid tautomer.

Amide tautomerization has been subject to some recently published theoretical studies on smaller amides.<sup>33–35</sup> Energetics for the water-assisted tautomerization reaction for Asn calculated in this study are in good agreement with these studies, which showed formamide tautomerization to be approximately 20 kcal/mol with water assistance.

**3b. Ring Closure of Amidic Acid Tautomer.** The amidic acid tautomer formed through tautomerization of the Asn side chain may undergo ring closure to yield the tetrahedral intermediate (Scheme 6). The energy required for a concerted ring closure starting from the amidic acid tautomer is approximately 27 kcal/mol in the gas phase, but the effect of a polar environment significantly reduces this barrier to 17.5 kcal/mol in solution (Figure 8).

A variant of the concerted ring closure mechanism with two peripheral water molecules was also modeled (Figure 9). These solvent molecules are not actively involved in the reaction; however, they lower the barrier by stabilizing the transition state through a hydrogen bond network.

Ring closure of the amidic acid tautomer can also occur through a stepwise mechanism with active water assistance (Figure 10). In the first step of the stepwise ring closure, the backbone NH proton is transferred to the Asn side chain through a water molecule, forming a zwitterionic intermediate, which then undergoes ring closure to form the tetrahedral intermediate. The overall free energy of activation for the stepwise ring closure of the amidic acid tautomer is 4.4 kcal/mol lower than the energy of the concerted ring closure with no water assistance (Figure 8).

The favorable interactions in Figure 9 and the stepwise mechanism in Figure 10, which prove to be helpful in reducing the activation barrier, have been combined to model the stepwise ring closure of the amidic acid tautomer with three peripheral water molecules (Figure 11), where only one of the water molecules is actively involved in the reaction mechanism. The three water-assisted ring closure mechanisms (Figures 9–11) have comparable barriers.

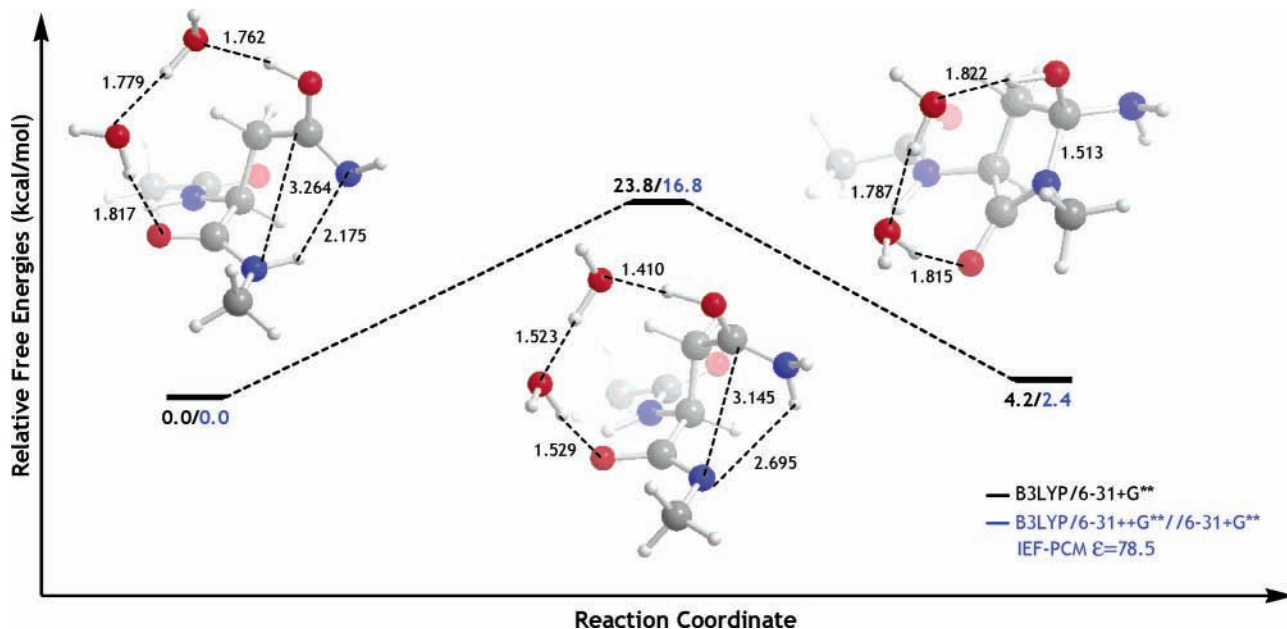


Figure 9. Potential free energy profile for the concerted ring closure in amidic acid tautomer with passive assistance of 2 H<sub>2</sub>O molecules.

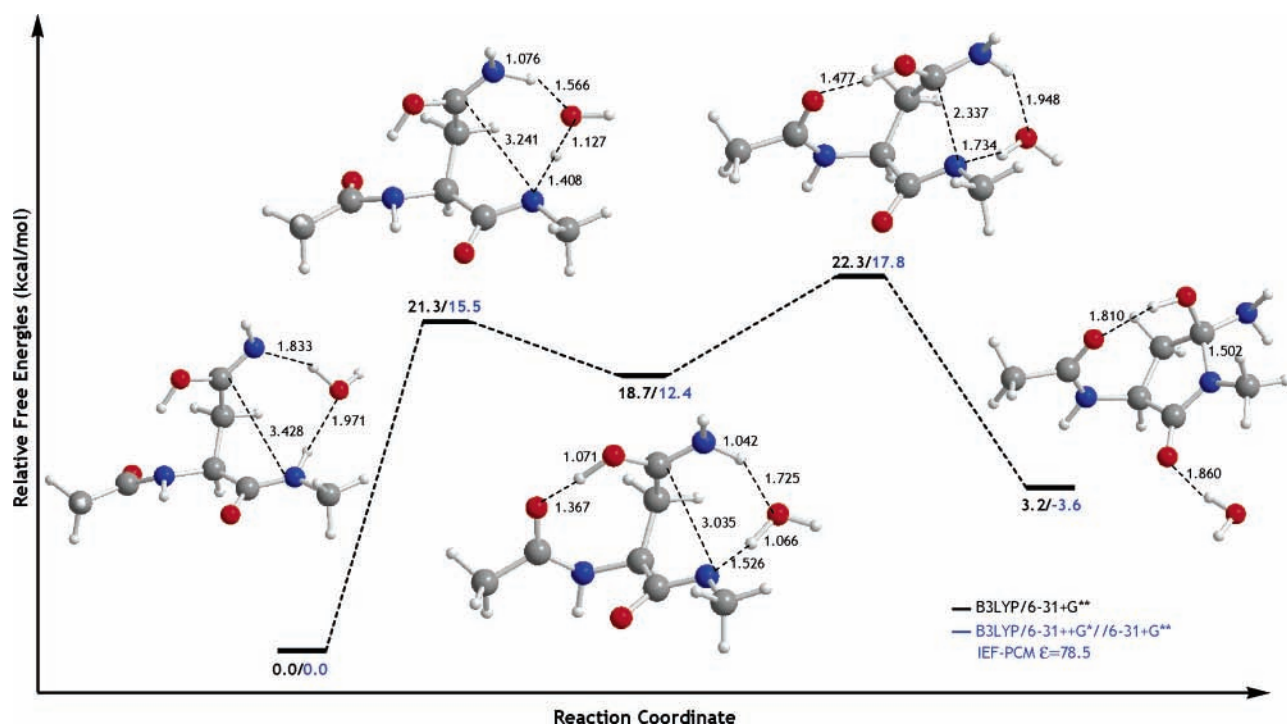


Figure 10. Potential free energy profile for the stepwise ring closure in amidic acid tautomer with active assistance of 1 H<sub>2</sub>O molecule.

It is imperative to indicate that the activation barriers associated with the ring closure of the amidic acid tautomer (Figures 8–11) cannot be directly compared with barriers of concerted (Figures 1–3) or stepwise (Figure 4) cyclizations. It should be noted that the amidic acid tautomer must first be formed before it can undergo a ring closure to give the tetrahedral intermediate. The mechanism and energetics for the formation of the amidic acid tautomers were previously shown in Figures 5–7. Hence, the reactants in Figures 8–11 are higher in energy than the reactants in Figures 1–4.

The concerted (Figure 3) and stepwise (Figure 4) water-assisted cyclization and the stepwise water-assisted ring closure of the amidic acid tautomer (Figure 11) have three peripheral H<sub>2</sub>O molecules, i.e., identical molecularities, enabling a legitimate comparison of the free energy of activation for these

mechanisms. The reactants in Figures 3 and 4 have similar geometries and are energetically almost identical. For an appropriate comparison of the energetics for these three mechanisms, the overall barrier for the mechanism in Figure 11 was reevaluated, taking the reactants of Figures 3 and 4 as the starting point. The overall barrier for the cyclization through the tautomerization route (Figure 11) starting from the reactants of Figures 3 and 4 was computed to be 33.4 kcal/mol. In light of this result, it is important to point out that the second step in both the stepwise water-assisted cyclization (Figure 4) and the stepwise water-assisted ring closure of the amidic acid tautomer (Figure 11) are identical. Whether the reactant undergoes a deprotonation/protonation followed by a backbone rotation (Figure 4) or a side chain tautomerization followed by a deprotonation/protonation step (Figure 11), it ends up at the



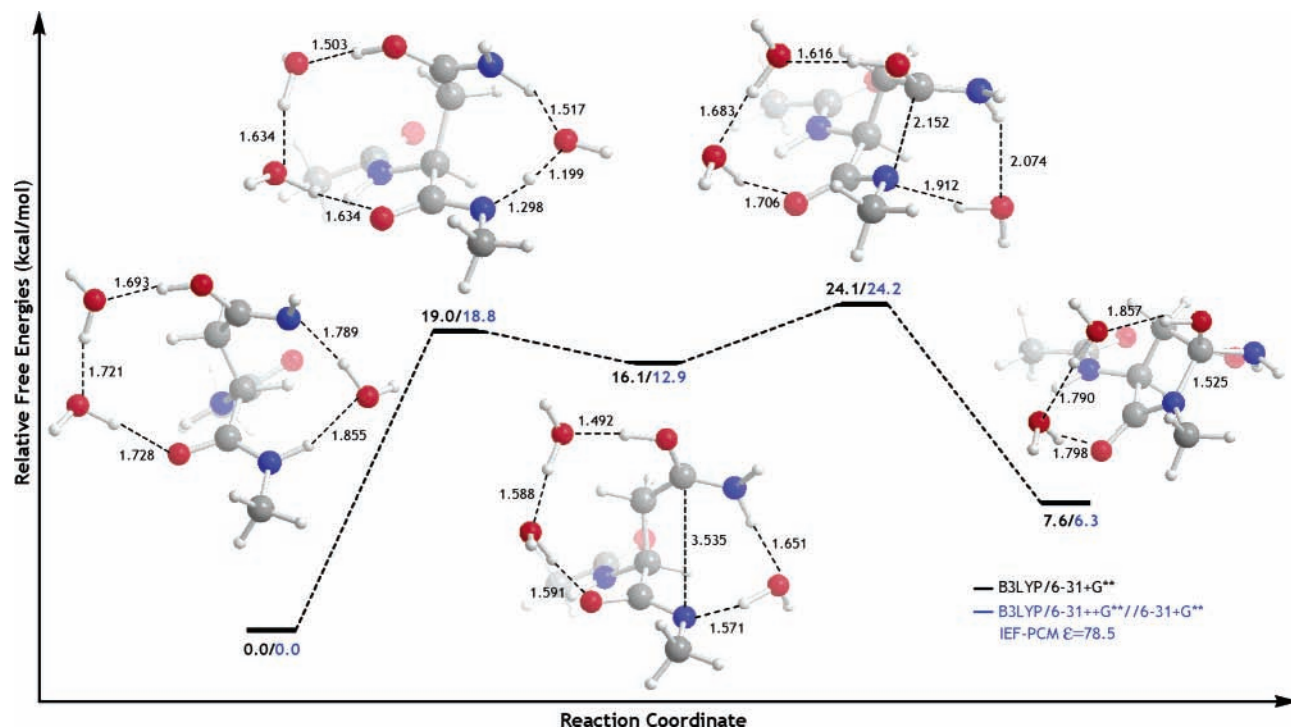


Figure 11. Potential free energy profile for the stepwise ring closure in amidic acid tautomer with active assistance of 2 H<sub>2</sub>O molecule

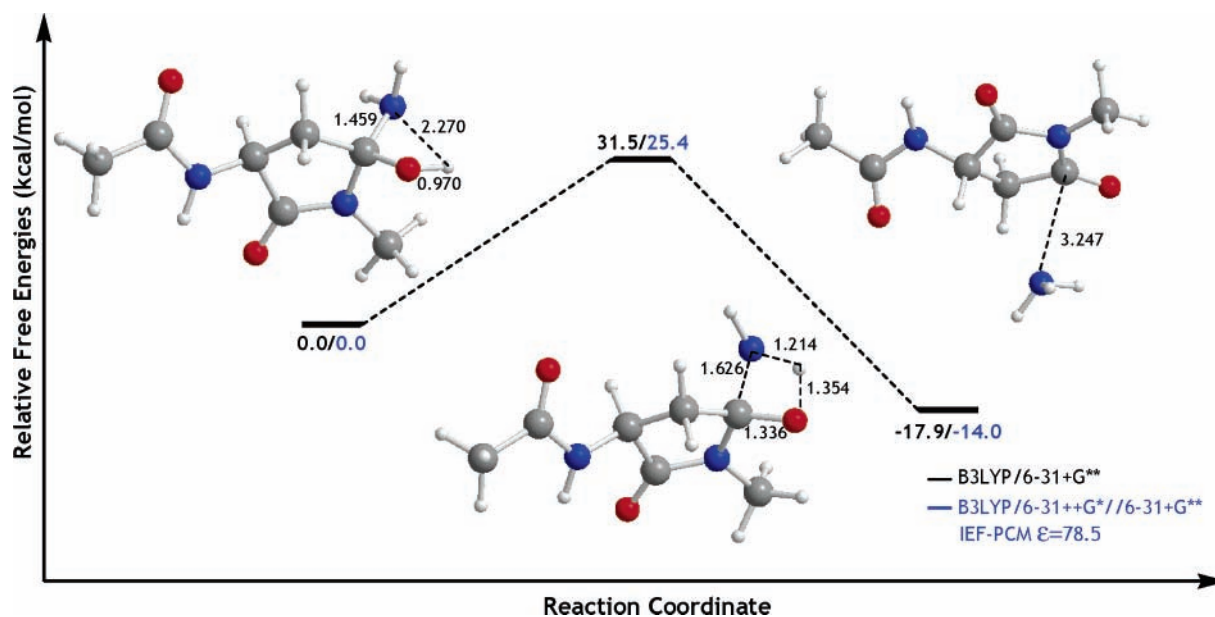
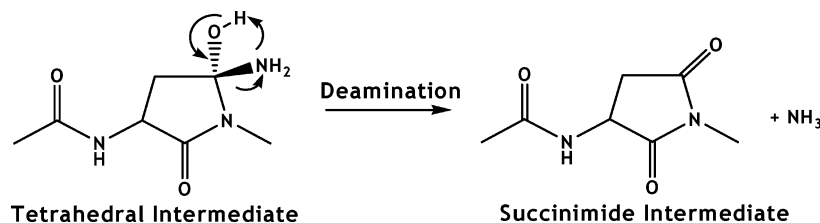


Figure 12. Potential free energy profile for the deamination without explicit H<sub>2</sub>O molecules.

**SCHEME 7: Deamination (Loss of NH<sub>3</sub>) in the Tetrahedral Intermediate To Yield the Succinimide Intermediate**



same zwitterionic intermediate, which explains the identical barriers of activation for these two mechanisms. However, it should be noted that the stepwise water-assisted cyclization mechanism (Figure 4) is probably less likely to occur, because the first step of this mechanism is highly reversible. The concerted water-assisted mechanism (Figure 3) has a slightly

higher barrier among the three mechanisms compared. As a result, the tautomerization route could be suggested to be the most probable mechanism for the formation of the tetrahedral intermediate. However, because the difference in activation energies are small, the most prominent outcome of these results is that all water-assisted mechanisms are more than 10 kcal/

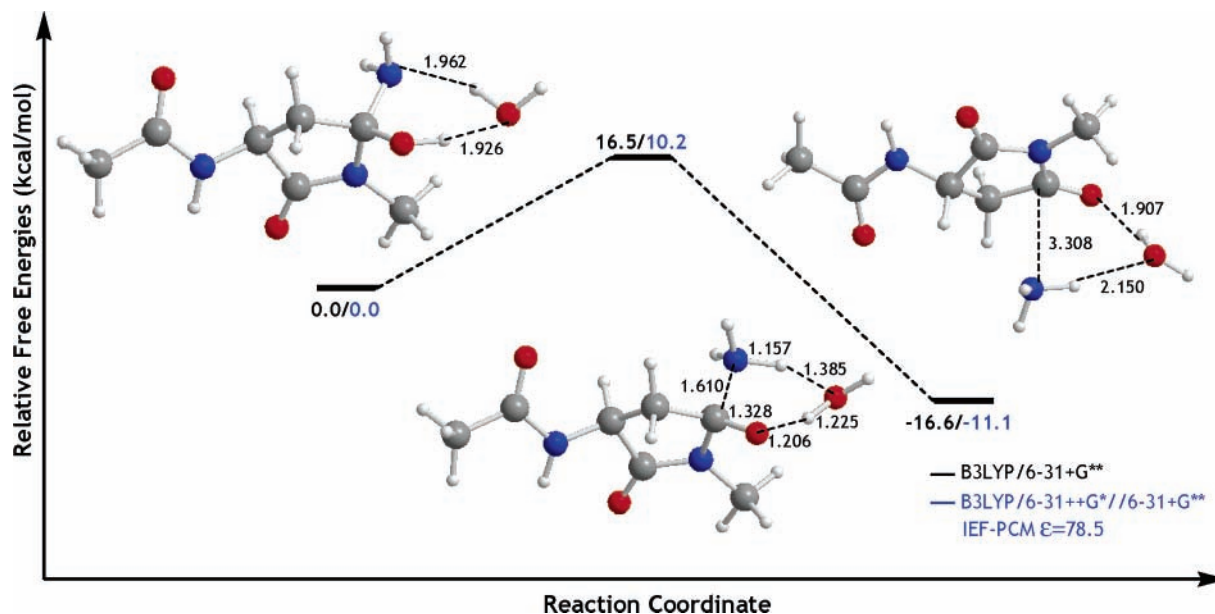


Figure 13. Potential free energy profile for the deamidation with 1 H<sub>2</sub>O molecule.

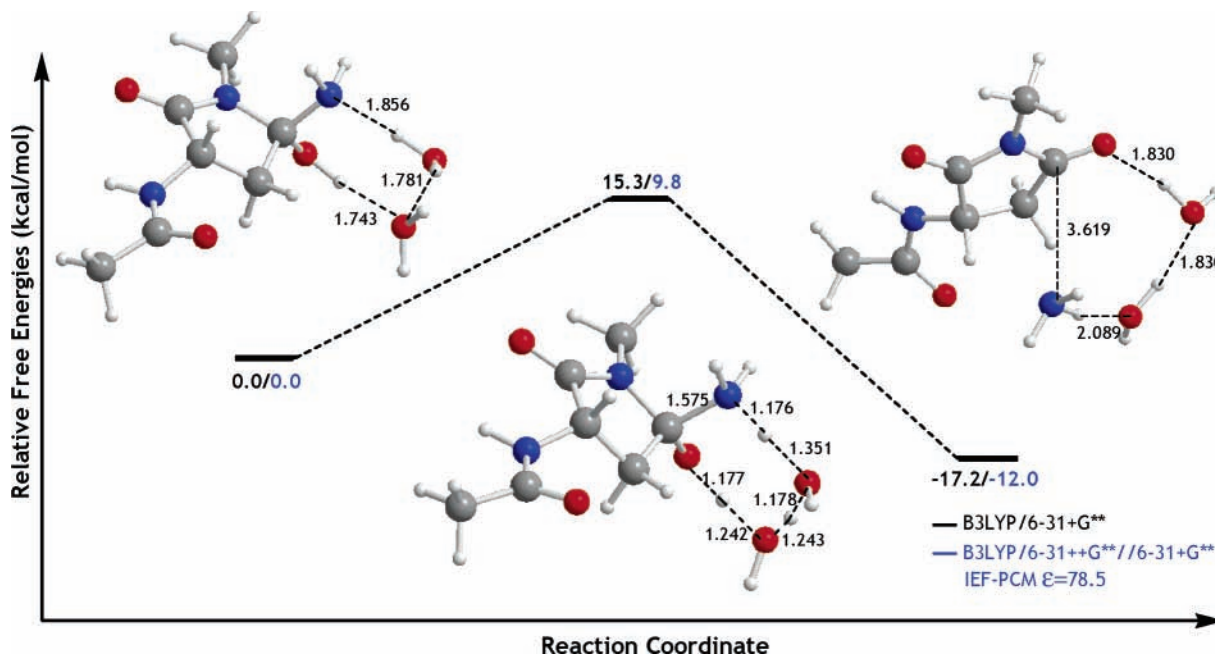


Figure 14. Potential free energy profile for the deamidation with 2 H<sub>2</sub>O molecules.

mol lower in energy than the previously proposed waterless concerted cyclization mechanism.<sup>14</sup>

**B. Deamidation.** The deamidation step is the loss of an NH<sub>3</sub> molecule from the tetrahedral intermediate to give the succinimide intermediate that Capasso et al. have previously proposed (Scheme 7). The NH<sub>2</sub> group in the tetrahedral intermediate was originally part of the amide functional group in the Asn side chain. The carbon atom bearing the -OH group is the carbonyl carbon of the Asn side chain, which has been protonated throughout the course of the reaction. A proton transfer from the -OH to the NH<sub>2</sub> causes consecutive departure of the amine (NH<sub>3</sub>). In addition, as the proton is abstracted a second C=O forms on the ring, expanding the surface for the delocalization of electrons through resonance. In this way, a much more stable intermediate known as the succinimide is formed.

The proton transfer may take place with or without the assistance of surrounding solvent molecules. However, proton

transfer through water molecules is expected to have a substantially lower barrier of activation, as shown throughout this study.

In this part of the study, the deamidation of the tetrahedral intermediate with no H<sub>2</sub>O assistance, as previously proposed,<sup>14</sup> has been reevaluated with the new model compound (Figure 12) and a higher basis set, similar to the case for the cyclization reaction. This is a concerted four-centered step with a barrier of 31.5 kcal/mol in gas phase. If deamidation is considered to go through a four-centered mechanism,<sup>14</sup> comparison of energetics between cyclization and deamidation suggests that deamidation may as well be the rate determining step in neutral media rather than the cyclization step. However, water-assisted deamidation mechanisms prove otherwise. The proton-transfer goes through a H<sub>2</sub>O molecule which is H-bonded to both the -NH<sub>2</sub> and the -OH involved in the reaction (Figure 13). The  $\Delta G^\ddagger$  for the one H<sub>2</sub>O-assisted deamidation in gas phase is half

that for the 4-centered mechanism (Figure 12). Furthermore, the activation barrier in solution for the one H<sub>2</sub>O-assisted deamination process is as low as 9.1 kcal/mol. The deamination process through two H<sub>2</sub>O molecules, in which the proton transfer takes place via two solvent molecules has also been explored (Figure 14). The energetics for both H<sub>2</sub>O-assisted deamination mechanisms are comparable. The exothermicity of the deamination reaction step is also noteworthy, indicating the stabilization in the ring.

Once the succinimide ring forms, the reversal to the Asn residue is considered not feasible. NH<sub>3</sub> attack on the succinimide ring is not foreseen, due to the negligibly small amount of NH<sub>3</sub> produced during the reaction. At this point, hydrolysis is inevitable and either an Asp or an iso-Asp residue will form.

## Conclusion

The aim of this study was to reinvestigate the energetics of the deamidation mechanism in peptides with the effect of solvent molecules, suggesting different pathways involving the assistance of explicit H<sub>2</sub>O molecules.

Three different mechanisms were suggested for the cyclization step of the deamidation reaction, which was previously proposed to be the rate determining step.<sup>14</sup> All water-assisted cyclization reactions investigated in this study were shown to have a significantly lower barrier than the previously proposed concerted waterless mechanism. Three water-assisted mechanisms with identical molecularities (Figures 3, 4 and 11) were shown to have overall barriers in the range 34–37 kcal/mol, approximately 15 kcal/mol lower in energy than the concerted waterless mechanism previously proposed. The most probable mechanism for the formation of the tetrahedral intermediate is proposed to be the tautomerization route; nevertheless, because the barrier differences between these three mechanisms is small, the other two should also be considered as competitive reaction pathways.

This study has established the effect of water molecules on the deamination step of the deamidation reaction, verifying that the cyclization step, with a substantially higher barrier for activation, is the rate determining step. It is also noteworthy that the involvement of water molecules in the deamination step has lowered the barrier to half.

This study has shown that water molecules in the vicinity of asparaginyl residues serve as a catalyst in deamidation reactions. Deamidation in proteins may as well be enhanced by other residues, which are capable of accepting or donating protons. However, experimental results have shown that the three-dimensional structure of the protein accelerates deamidation in only 6% of the cases.<sup>7,36</sup> Therefore, one may conclude that deamidation in proteins or enzymes will be more probable for those potential deamidating sites that exhibit the largest accessibility by solvent molecules.

This investigation also suggests that a quantitative description of the process may require carrying out a detailed statistical treatment of the solvent effect. This will be done in future studies using molecular dynamics simulations and combined QM/MM potentials. Further investigations will also include examination of (1) solvent-assisted mechanisms in enzymes having sites with different deamidation rates and (2) the effect of the identity of the  $n + 1$  residue on deamidation, which is known to have different half-times for different amino acids.

**Acknowledgment.** S.C. thanks the French Embassy in Ankara, Turkey, for the co-tutelle grant in France and the TUBITAK National Ph.D. scholarship. We thank CINES

(Centre Informatique National de l'Enseignement Supérieur) for computer facilities (Project No. lct2636) and acknowledge the TUBITAK High Performance Computing Center for computational resources. S. Catak would also like to express gratitude to Dr. B. Balta, for fruitful discussions during the course of this study. V.A. would like to dedicate this article to the memory of Chava Lifshitz, the brilliant scientist and wonderful person, for being her mentor in her academic life since 1985. The guidance Chava Lifshitz provided as a dedicated and meticulous scientist will continue to inspire V.A. and her students in their future research and academic life.

## References and Notes

- (1) Robinson, A. B.; Rudd C. *Curr. Top. Cell Regul.* **1974**, *8*, 247–295.
- (2) Robinson, A. B.; Scothler, J. W.; McKerrow, J. H. *J. Am. Chem. Soc.* **1973**, *95*, 8156–8159.
- (3) Robinson, N. E.; Robinson, A. B. *Molecular Clocks: Deamidation of Asparaginyl and Glutaminyl Residues in Peptides and Proteins*; Althouse Press: Cave Junction, OR, 2004.
- (4) Gupta, R.; Srivastava, O. P. *J. Biol. Chem.* **2004**, *279*, 44258–44269.
- (5) Solstad, T.; Carvalho, R. N.; Anderson, O. A.; Waidelich, D.; Flatmark, T. **2003**, *Eur. J. Biochem.* *270*, 929–938.
- (6) Kim, E.; Lowenson, J. D.; MacLaren, D. C.; Clarke, S.; Young, S. G. *Proc. Natl. Acad. Sci. U.S.A.* **1997**, *94*, 6132–6137.
- (7) Robinson, N. E.; Robinson, A. B. *Proc. Natl. Acad. Sci. U.S.A.* **2001**, *98*, 12409–12413.
- (8) Weintraub, S. J.; Manson, S. R. *Mech. Age. Dev.* **2004**, *125*, 255–257.
- (9) Robinson, N. E.; Robinson, A. B. *Proc. Natl. Acad. Sci. U.S.A.* **2001**, *98*, 944–949.
- (10) Capasso, S.; Mazzarella, L.; Sica, F.; Zagari, A.; Salvadori, S. *J. Chem. Soc. Chem. Commun.* **1992**, 919–921.
- (11) Capasso, S.; Mazzarella, L.; Sica, F.; Zagari, A.; Salvadori, S. *J. Chem. Soc., Perkin Trans. 2* **1993**, 679–682.
- (12) Capasso, S.; Salvadori, S. *J. Peptide Res.* **1999**, *54*, 377–382.
- (13) Capasso, S.; Mazzarella, L.; Sica, F.; Zagon, A. *J. Peptide Res.* **1989**, *2*, 195–197.
- (14) Konuklar, F. A.; Aviyente, V.; Sen, T. Z.; Bahar, I. *J. Mol. Model.* **2001**, *7*, 147–160.
- (15) Konuklar, F. A.; Aviyente, V. *Org. Biomol. Chem.* **2003**, *1*, 2290–2297.
- (16) Konuklar, F. A.; Aviyente, V.; Ruiz-Lopez, M. F. *J. Phys. Chem. A* **2002**, *106*, 11205–11214.
- (17) Robinson, N. E.; Robinson, A. B. *J. Peptide Res.* **2004**, *63*, 437–448.
- (18) Stewart, J. J. P. *J. Comput. Chem.* **1989**, *10*, 221–264.
- (19) Parr, R. G.; Yang, W. *Density-functional theory of atoms and molecules*; Oxford University Press: Oxford, U.K., 1989.
- (20) Hohenberg, P.; Kohn, W. *Phys. Rev.* **1964**, *136*, B 864.
- (21) Kohn, W.; Sham, L. *J. Phys. Rev.* **1965**, *A* 1133.
- (22) Becke, A. D. *J. Chem. Phys.* **1993**, *98*, 5648–5652.
- (23) Lee, C.; Yang, W.; Parr, R. G. *Phys. Rev.* **1988**, *B37*, 785.
- (24) Madura, J.; Jorgensen, W. L. *J. Am. Chem. Soc.* **1986**, *108*, 2517–2527.
- (25) Gonzalez, C.; Schlegel, H. B. *J. Chem. Phys.* **1989**, *90*, 2154–2161.
- (26) Gonzalez, C.; Schlegel, H. B. *J. Phys. Chem.* **1990**, *94*, 5523–5527.
- (27) Tomasi, J.; Mennucci, B.; Cancès, E. *J. Mol. Struct. (THEOCHEM)* **1999**, *464*, 211–226.
- (28) Cancès, M. T.; Mennucci, B.; Tomasi, J. *J. Chem. Phys.* **1997**, *107*, 3032–3041.
- (29) Mennucci, B.; Tomasi, J. *J. Chem. Phys.* **1997**, *106*, 5151–5158.
- (30) Mennucci, B.; Cancès, E.; Tomasi, J. *J. Phys. Chem. B* **1997**, *101*, 10506–10517.
- (31) Bondi, A. *J. Phys. Chem.* **1964**, *68*, 441–451.
- (32) Frisch, M. J.; Trucks, G. W.; Schlegel, H. B.; Scuseria, G. E.; Robb, M. A.; Cheeseman, J. R.; Montgomery, J. A., Jr.; Vreven, T.; Kudin, K. N.; Burant, J. C.; Millam, J. M.; Iyengar, S. S.; Tomasi, J.; Barone, V.; Mennucci, B.; Cossi, M.; Scalmani, G.; Rega, N.; Petersson, G. A.; Nakatsuji, H.; Hada, M.; Ehara, M.; Toyota, K.; Fukuda, R.; Hasegawa, J.; Ishida, M.; Nakajima, T.; Honda, Y.; Kitao, O.; Nakai, H.; Klene, M.; Li, X.; Knox, J. E.; Hratchian, H. P.; Cross, J. B.; Bakken, V.; Adamo, C.; Jaramillo, J.; Gomperts, R.; Stratmann, R. E.; Yazyev, O.; Austin, A. J.; Cammi, R.; Pomelli, C.; Ochterski, J. W.; Ayala, P. Y.; Morokuma, K.;

Voth, G. A.; Salvador, P.; Dannenberg, J. J.; Zakrzewski, V. G.; Dapprich, S.; Daniels, A. D.; Strain, M. C.; Farkas, O.; Malick, D. K.; Rabuck, A. D.; Raghavachari, K.; Foresman, J. B.; Ortiz, J. V.; Cui, Q.; Baboul, A. G.; Clifford, S.; Cioslowski, J.; Stefanov, B. B.; Liu, G.; Liashenko, A.; Piskorz, P.; Komaromi, I.; Martin, R. L.; Fox, D. J.; Keith, T.; Al-Laham, M. A.; Peng, C. Y.; Nanayakkara, A.; Challacombe, M.; Gill, P. M. W.; Johnson, B.; Chen, W.; Wong, M. W.; Gonzalez, C.; Pople, J. A. *Gaussian 03*, revision B.05; Gaussian, Inc.: Wallingford CT, 2004.

(33) Liang, W.; Li, H.; Hu, X.; Han, S. *J. Phys. Chem. A* **2004**, *108*, 10219–10224.

(34) Hazra, M. K.; Chakraborty, T. *J. Phys. Chem. A* **2005**, *109*, 7621–7625.

(35) Du, D.; Fu, A.; Zhou, Z. *Int. J. Quantum Chem.* **2004**, *99*, 1–10.

(36) Robinson, N. E.; Robinson, A. B. *Proc. Natl. Acad. Sci. U.S.A.* **2001**, *98*, 4367–4372.